THE MODIFICATION AND DEVELOPMENT OF THE SPECTROSCOPIC PROPERTIES OF Cs/PVA BLEND INCORPORATED GOLD NANOPARTICLES (AuNPs) PREPARED BY PULSED LASER ABLATION IN LIQUIDS (PLAL)

L. H. GAABOUR[*], K. A. HAMAM
University of Jeddah, College of Science, Department of Physics, Jeddah, Saudi Arabia

In the present work, pure gold nanoparticles (AuNPs) were synthesis by pulsed laser ablation technique using Nd:YAG as a source of laser. Then, the prepared AuNPs was used with low concentrations to synthesis nanocomposite films by adding it to chitosan/polyvinyl alcohol (Cs/PVA) blend using the casting method. All peaks of pure AuNPs were recorded by X-ray diffraction with face center cubic (FCC) structure. No peaks of AuNPs were found at low concentrations in the doped nanocomposites because of the complete degradation of AuNPs within Cs/PVA matrix. The intensity of some IR bands was changed due to the chemical interaction between the components. The broad band at 3350 cm^{-1} was decreased due to the intermolecular interaction. Dielectric constant and dielectric loss were decreased as an increase in the frequency and temperature. The increases of direct conductivity (σ_{dc}) imply that the free charge density or of the charge mobility that results. The AuNPs addition assists the charge transfer complex (CTCs) formation in which charge transportation occurs by coulomb forces and electric field. The Cole-Cole plot shows semicircles that supports the relaxation processes were a non-Debye method.

1. Introduction

Gold nanoparticles get high importance among metal nanoparticles, regardless of their ability to communicate with light primarily through the surface Plasmon resonance (SPR) [1]. AuNPs are now very prominent in many technologies because of their incredible characteristics, such as; catalytic, electrical, and mechanical [2].

Polymer blending, which is well established as polymer mixing, is now making a strong effort to develop new polymeric material with a variety of qualities and abroad uses [3, 4]. The subsequent new polymer blend product has special, not-fine characteristics in every single polymer. Nanoparticles doped polymers as a nanocomposite were interested in receiving a new approach for introducing a new material with the required characteristics that are significant in terms of different characteristics [5, 6].

Chitosan (CS) is a natural polysaccharide and a cationic polymer [7, 8]. It may be produced from chitin extracted from shrimp shells and recommended for a wide range of applications, including use of medicinal, biomedical and food support due to its accessibility, biocompatibility, biodegradability, non-toxicity and antifungal activity, gas and aroma barriers. However, before breakage, pure chitosan has a low elongation ratio that can impede its application. One of the best possibilities to overcome this obstacle could, therefore, be accomplished by combining CS with other inorganic compounds such as polyvinyl alcohol (PVA) [9-11].

PVA is a semi-crystalline polymer comprising hydroxyl groups (O – H) [12, 13]. It has been recommended for various applications, including electrical and medical applications, due to its high tensile strength and durability, non-toxicity, degradability, water-solubility, a strong

---

[*] Corresponding author: lhgaabour@uj.edu.sa

capacity for storage, reduction efficiency, high dielectric constant, in addition to great optical properties. The purpose of this article is to modification and development of the spectroscopic and electrical properties of chitosan/polyvinyl alcohol (Cs/PVA) blend incorporated gold nanoparticles (AuNPs) prepared by pulsed laser ablation in liquids (PLAL). The obtained data from the analysis confirmed that the nanocomposites are used in different applications like electronic devices.

2. Experimental section

2.1. Preparation of gold nanoparticles (AuNPs)

Pure gold nanoparticles (AuNPs) were synthesized using pulsed laser ablation in liquids (PLAL) technique as the following steps. Firstly, a specimen of high purity gold (Au) with dimensions 4 mm x 4 mm x 1 mm was used. The gold sample was then polished in a beaker have 20 ml of double-distilled water. The gold ample has suitable dimensions. Pure gold sample was polished and is then washed several times with double distilled water, pure alcohol and then dried. Laser beam was focused vertically on the target sample. The gold sample was immersed in approximately 15 mm of pure water in a beaker. Then, the nanoscale gold granules were obtained by laser pulses after a specified period of time. Laser beam with a laser wavelength λ = 1064 nm was projected on the sample. The laser beam pulse has 6 ns time intervals, at a frequency of 10 Hz.

2.2. Preparation of the (Cs/PVA-AuNPs) nanocomposites

Chitosan (Cs) have low molecular weight and polyvinyl alcohol (PVA) with molecular weight 140000 g/mol. All the polymers were supplied from Sigma-Aldrich company. The weight ratio between the polymers was Cs:PVA (80/20 wt./wt.). The Cs/PVP nanocomposite samples containing 2, 4, 8 and 12 ml of AuNPs were prepared by the solution casting method as the following procedures. 4 grams of chitosan (Cs) and one gram of PVA was dissolved in double-distilled water separately. The total solution of Cs/PVA blend was mixed and stirred at 60 °C for about 6 h. The amount of the gold nanoparticle solution was added drop by drop to Cs/PVA solution with stirring about 30 min. The final solution of each concentration of the Cs/PVA–AuNPs was cast in Petri dishes and left in an oven at three days at 47 °C to evaporate the solvent and kept about 15 min to prevent any bubbles. The obtained films of Cs/PVP–AuNPs nanocomposites were stored in a desiccator until uses. The thickness of the nanocomposites in nearly 200 μm and the Cs/PVP films was colourless and the samples contain AuNPs were brown-yellow colour.

2.3. The measurements

The X-ray diffraction (XRD) analysis was carried out by X'Pert[3] Powder with CuKα radiation at λ = 1.5406 Å with 2θ = 5°–80°. Fourier transform infrared (FT-IR) measurements were carried out by a Bruker VERTEX 70 IR–Fourier spectrometer. The spectra were recorded in the Attenuated Total Reflectance (ATR) mode in the range of 4000- 400 cm-1 using a resolution of 0.4 cm^{-1}. The AC electrical conductivity measurements were carried out using broadband dielectric spectroscopy type (concept 40) Novocontrol High-Resolution Alpha Analyzer supported by Quatro Temperature Controllers using nitrogen as heating agent with the range of frequency from 100 Hz to 7 MHz and at different of temperature from 25 °C to 120 °C. range 25–125 °C.

3. Results and discussion

3.1. The X-ray diffraction (XRD)

The X-ray diffraction (XRD) spectra of Cs/PVA doped with 0, 4, 8 and 12 ml of AuNPs is shown in Fig. 1. The XRD spectrum of synthesis AuNPs is inserted inside figure 1. The main peaks for the AuNPs are recorded as in the spectrum as: at 2 θ = 38.51, 44.12, 64.31 and 77.14° which are related to Bragg reflections (111), (2000), (220) and (311), respectively. The appearance of these peaks for the Au spectrum depicts face centered cubic (FCC) structure. This is consistent

with the standard card (JCPDS file No. 04-0784) [14. 15]. Further, the crystallite size of these AuNPs is determined using the formula of Debye–Scherer's [16, 17] for the (111) planes at $2\theta = 38.51°$.
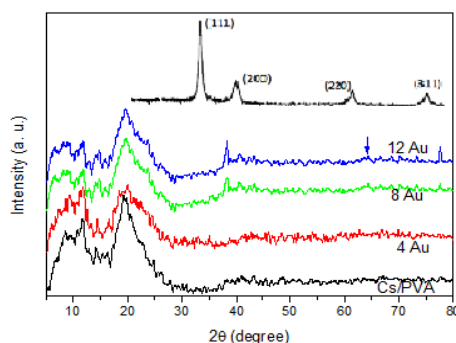
Fig. 1. The X-ray diffraction of the Cs/PVA polymer blend incorporated by 0, 4, 8 and 12 ml gold nanoparticles (AuNPs).

On the other hand, the two broad (hump) diffraction peaks are centered at $2\theta = 11.74°$ and $19.49°$ which confirm the semicrystalline nature of pure Cs/PVA blend [18]. All characteristic peaks of pure AuNPs are founded in the samples (8 and 12 ml), which depicts the presence of the nanoparticle phases within the Cs/PVA polymeric matrices. No peaks of AuNPs are observed at low concentrations due to the complete degradation of the AuNPs within the Cs/PVA matrix. But at the higher concentrations of AuNPs (8 and 12 ml), the peaks of the nanogold are observed in the near position attributed to the existence of AuNPs in Cs/PVA polymeric matrix.

Depending on the AuNPs concentration, the intensity of the main broad peaks is decreased, implying the reduction of the crystallinity degree of nanocomposite samples. These data are attributed to the complexation and interaction between the nanogold and the Cs/PVA structure that results in a disruption of Cs/PVP crystalline structure. Further, the reduction in the intensities of main halos indicates that the embedded AuNPs exist within the structures of nanocomposite films and their electrostatic interactions disrupt the crystalline phases of the Cs/PVA matrix. These observations depict the suitability of nanocomposite samples for the development of solid polymer electrolytes since the decrease of crystallinity is needed in the ionic conductivity enhancement in solid ion-dipolar complexes.

3.2. The ATR-FTIR analysis

The attenuated total reflectance-Fourier transform infrared spectroscopy (ATR-FTIR) spectra of pure Cs, pure PVA and pure Cs/PVA blend are shown in Fig. 2 and Fig. 3 shows the FT-IR of Cs/PVA doped with different concentrations of AuNPs. The ATR-FIIR bands of pure Cs are assigned as [19, 20]: the broad band is observed at 3353 cm^{-1} which is attributed to OH group and the band at 3903 cm^{-1} is assigned to NH_2 stretching vibrations. The IR band at 1646 cm^{-1} is assigned to $C = O$ group of (amide I) and at 1565 cm^{-1} is due to N-H bending mode (amide II). The IR bands observed at 1403 cm^{-1} and 1373 cm^{-1} are attributed to C-H bending group and the band at 1312 cm^{-1} is assigned to C-N groups. The bands related to C-O stretching from the glycosidic bonds are seen at 1150 cm^{-1}, 1039 cm^{-1} and 1020 cm^{-1} and the bands at 900 cm^{-1} and at 604 cm^{-1} are related to C-H wagging vibration of Cs saccharide structure.
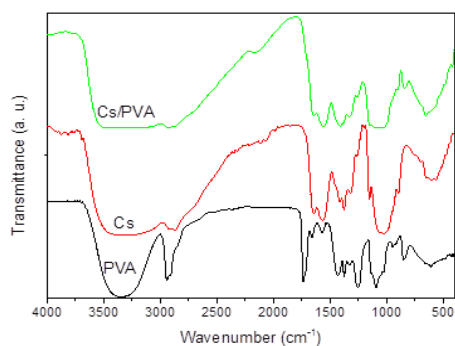
Fig. 2. The ATR- FTIR transmittance spectra of pure Cs, pure PVA and Cs/PVA polymer blend.
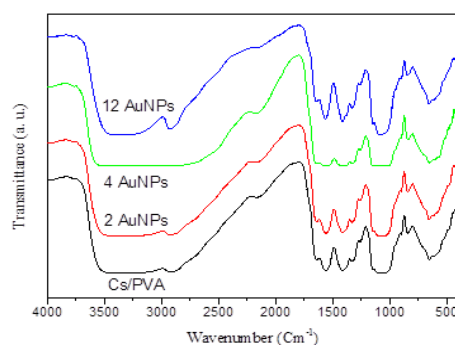
Fig. 3. The ATR- FTIR transmittance spectra of the Cs/PVA polymer blend incorporated by 0, 4, 8 and 12 ml gold nanoparticles (AuNPs).

The FI-IR bands of pure PVA are assigned as [21, 22]: The broad band at 3344 cm^{-1} is assigned to OH symmetric stretching mode and the band at 2939 cm^{-1} is related to C-H asymmetric stretching vibrational mode. The sharp IR bands which observed at 1723 cm^{-1} and 1650 cm^{-1} are due to C=O and C = C stretching vibrational mode, respectively. Two IR bands which seen at 1431 cm^{-1} and at 1379 cm^{-1} are related to C-H bending and C-H wagging vibrational mode, respectively. The IR band at 1259 cm^{-1} is assigned to C–H wagging vibrational mode of acetate residue and the band at 1098 cm^{-1} is related to C-O stretching vibrational mode but the band at 841 cm^{-1} is assigned to CH$_2$ rocking vibrational mode.

The spectrum of pure Cs/PVA polymer blend display a broad band at 3303 cm^{-1} is attributed to OH vibrational mode and the band at 2908 cm^{-1} is related to C–H stretching from pyranose rings. The two bands are observed at 1643 cm^{-1} and at 1562 cm^{-1} are assigned to C=O and N–H bonding and the band at 1176 cm^{-1} is related to C–C vibrational mode [23]. A little decrease in the intensities of some bands is occurred due to the presence of the hydrogen bond between OH and/or NH$_2$ groups in Cs and OH in PVA as we see in Scheme 1.

After the addition of the gold nanoparticles, the broad band centered at 3350 cm^{-1} which attributed to hydrogen bond between OH and NH$_2$ functional groups is decreased because of the intermolecular interaction between polymer blend and the AuNPs through the formation of coordination interactions with the –OH, C=O group of acetate group and C=O group of the amide group. The obtained observations of these reactions are confirmed by X-ray analysis attributed to the increase of the amorphous region inside the polymeric matrix.

3.3. AC electrical conductivity
3.3.1. The dielectric permittivity
Figs. 4 and 5 show the dielectric constant (ε') and dielectric loss (ε'') as a function of the frequency (Log f) at room temperature of Cs/PVA incorporated 0, 4, 8 and 12 ml of gold

nanoparticles (AuNPs) in frequencies range 100 Hz-7 MHz. Form the figures, the values of both ε' and ε'' are decreased when the frequency increased for all the samples. This behaviour is due to the high contribution of charge accumulation inside the nanocomposite samples or attributed to the direction of the dipoles inside the nanocomposites to orient in direction of the applied field. The nonlinearity at the intermediate frequency is related to the dipolar polarization inside chain segments between the polymeric matrices. In the higher frequency range, the trend of the decrease is nearly stable. The periodic reversal of the electric field occurs so fast that there is no excess ion diffusion in the direction of the field. Hence the polarization due to charge accumulation decreases and results in a decrease in both the ε' and ε'' values.
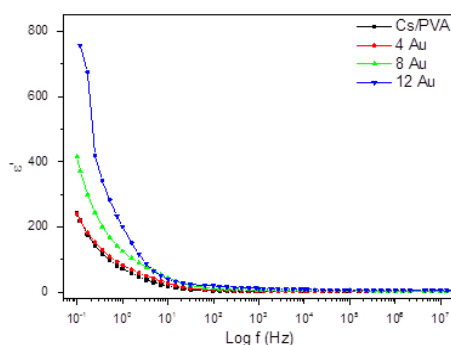
Fig. 4. The variation of the dielectric constant (ε') with the frequency of the Cs/PVA polymer blend incorporated by 0, 4, 8 and 12 ml gold nanoparticles (AuNPs).
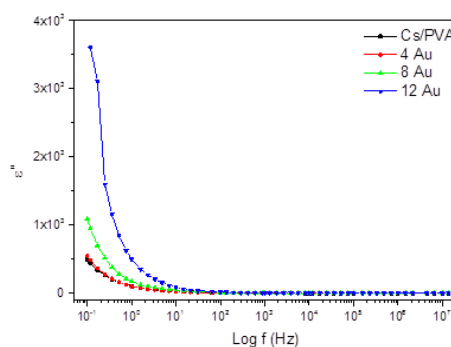
Fig. 5. The variation of the dielectric loos (ε'') with the frequency of the Cs/PVA polymer blend incorporated by 0, 4, 8 and 12 ml gold nanoparticles (AuNPs).

Fig. 6 and 7 represent the (ε' and ε'') as a function of the frequency at different temperatures (30, 60, 90 and 120 °C) of Cs/PVA doped with 12 ml of AuNPs. At low frequencies and high temperatures, we see that high values of dielectric permittivity are involved in dipole direction, conduction sharing, and the effect of Maxwell-Wagner-Sillars with the polarization. Two types of transformations that can be recorded here as follows: with increasing frequency and the increase in different temperatures, and with each shift corresponds to a sudden decrease in dielectric permittivity. This indicates that the segmental dipole is the one that often contributes to the extent of the buffer response of the nanocomposites. In the other type: there is one type of polar dipoles in the crystalline region, working to restrict in the direction of the dipoles by the crystal network, while the other dielectric constant and the loss of electrical insulation with temperature can increase the density of the charging carrier due to increased dissociation ionic groups.
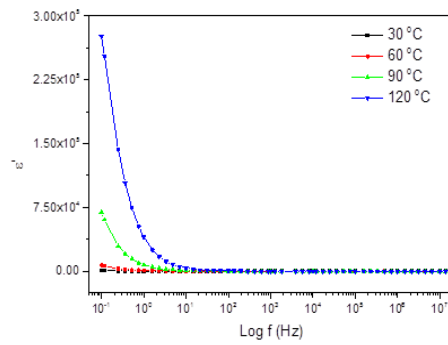
Fig. 6. The variation of the dielectric constant (ε') with the frequency of the Cs/PVA polymer blend incorporated by 12 ml gold nanoparticles (AuNPs) at 30, 60, 90 and 120 °C.
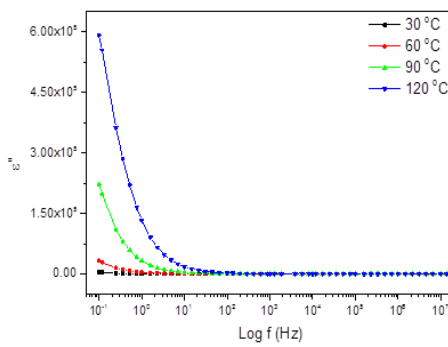
Fig. 7. The variation of the dielectric loss (ε'') with the frequency of the Cs/ polymer blend incorporated by 12 ml gold nanoparticles (AuNPs) at 30, 60, 90 and 120 °C.

3.3.2. Electrical conductivity

Fig. 8 shows the Log (σ') dependence on Log (f) of the virgin blend of Cs/PVA and the prepared nanocomposite films at room temperature.
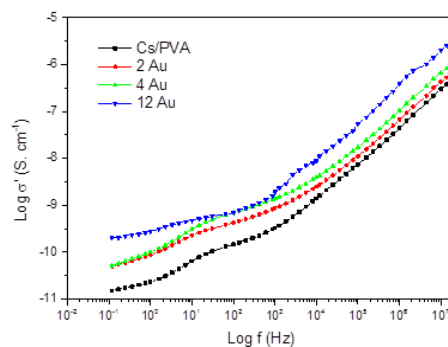
Fig. 8. The variation of the real part of conductivity (σ'_{ac}) with the frequency of the Cs/PVA polymer blend incorporated by 0, 4, 8 and 12 ml gold nanoparticles (AuNPs).

It is obvious that the values of σ′ increase linearly with of the frequency increase and show distinguishable dispersion behaviour over the audio/radio frequency regions, which are referred to the semicrystalline nature of these samples. Further, the σ′ values follow the Jonscher's power law [24]:

$$\sigma'(\omega) = \sigma_{dc} + A\omega^n \tag{1}$$

where, σ_{dc} is the dc electrical conductivity and *n* is the power law fit. The determined σ_{dc} values for these samples are recorded in Table 1. The σ_{dc} values of these nanocomposite materials gradually decrease with the increase of AuNPs. The increase in the σ_{dc} values of the nanocomposite films implies that there is either the increase of the free charge density or of the charge mobility that is a result of Cs/PVA polymer-AuNPs interactions. Also, the AuNPs addition assists the charge transfer complex (CTCs) formation in which charge transportation occurs by coulomb forces and electric field.

Table 1. The AuNPs concentration dependent on the conductivity and the dc electrical conductivity (σ_{dc}) at room temperature and also for Cs/PVA–12 ml AuNPs film at different temperatures.

sample	$\sigma^{'}$ (S.cm^{-1})	σ_{dc} (S.cm^{-1})
Cs/PVA	5.85×10^{-7}	4.97×10^{-16}
2 ml AuNPs	1.04×10^{-6}	5.63×10^{-16}
4 ml AuNPs	1.47×10^{-6}	1.23×10^{-15}
12 ml AuNPs	3.39×10^{-6}	2.45×10^{-15}

Cs/PVA–12 ml AuNPs

T (°C)	$\sigma^{'}$ (S.cm^{-1})	σ_{dc} (S.cm^{-1})
30 °C	5.85×10^{-7}	4.97×10^{-16}
60 °C	5.08×10^{-6}	9.37×10^{-15}
90 °C	6.76×10^{-6}	2.05×10^{-14}
120 °C	7.83×10^{-6}	6.02×10^{-14}

Also, Fig. 9 shows the frequency of Log (σ') on Log (f) for the virgin blend of Cs/PVA-12 ml AuNPs film at various temperatures. From this figure and Table 1, it is observed that there is a significant increase of σ' and σ_{dc} values with the increase of the temperature of the nanocomposite sample. This indicates that the electrical conduction is thermally activated, and the electrical mobility/number of free charge carriers increases with the temperature increase.
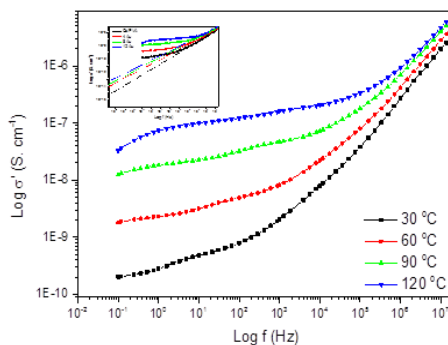
Fig. 9. The variation of the real part of conductivity (σ'_{ac}) with the frequency of the Cs/PVA polymer blend incorporated by 12 ml gold nanoparticles (AuNPs) at 30, 60, 90 and 120 °C.

3.3.3. Complex modulus
The mathematical equation complex modulus (M*) can be evaluated as [25, 26]:

$$M^{*} = M^{'} - jM^{''} = \frac{1}{\varepsilon^{*}} = \frac{\varepsilon^{'} + j\varepsilon^{''}}{(\varepsilon^{'})^2 + (\varepsilon^{''})^2} \qquad (2)$$

where, M' and M" are the real modulus (M′) and imaginary modulus (M″). The M′ and M″ are calculated as:

$$M' = \frac{\varepsilon'}{(\varepsilon'^2 + \varepsilon''^2)} \tag{3}$$

Fig. 10 shows the relation between the (M') with Log (f) at room temperature. The values of M' are increased with the increase of frequency an AuNPs content causing an increase of the ionic conduction of the samples. Fig. 11 shows the graph between the (M'') and Log (f) at room temperature. It is found that M' values increase non-linearly with an increase of frequency, whereas M'' spectra of these films show an electric modulus relaxation peak that is attributed to the polymeric motion of Cs/PVA chains. This peak is shifted toward high frequencies with the increase of AuNPs content, which indicates that the electrostatic interactions between the functional dipolar groups of Cs/PVA and AuNPs induce more flexibility to the polymer chain segmental dynamics. These findings confirm that there is a good dispersion of AuNPs within the Cs/PVA structure.
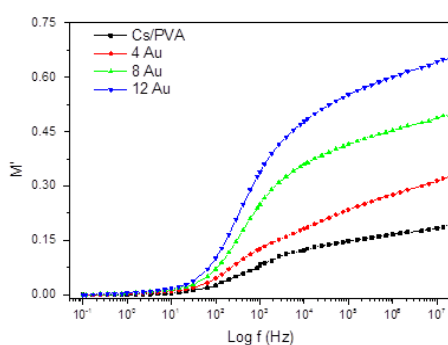
Fig. 10. The variation of M' with the frequency of the Cs/PVA polymer blend incorporated by 0, 4, 8 and 12 ml gold nanoparticles (AuNPs).
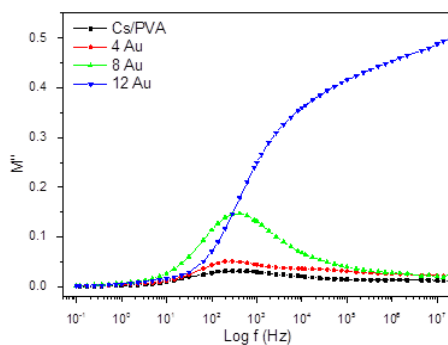
Fig. 11. The variation of M'' with the frequency of the Cs/PVA polymer blend incorporated by 0, 4, 8 and 12 ml gold nanoparticles (AuNPs).

For more understanding of the dielectric relations of the prepared samples and explore the nature of relaxation processes, Argand plot (M' versus M") are shown in Fig. 12. All spectra show a semicircle arc implying the presence of single relaxation processes i.e. Debye type relaxation process. Also, the radii of these semicircles decrease with the increase of AuNPs content, which indicates the increase of ionic mobility and so the electrical conductivity improvement.
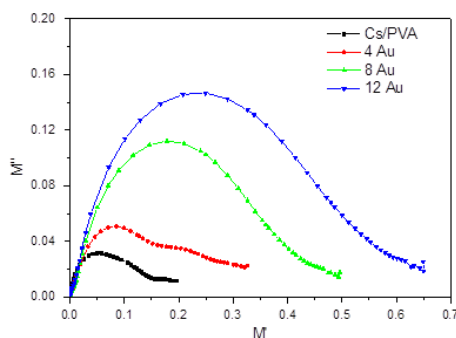
*Fig. 12. The variation between M' and M'' of the Cs/PVA polymer blend incorporated
by 0, 4, 8 and 12 ml gold nanoparticles (AuNPs).*

Fig. 13 shows the plot between the (M′) with Log (f) of Cs/PVA doped 12 ml of AuNPs at
30, 60, 90 and 120 °C. The values of M′ are increased with the increase of temperature causing
more increase of the ionic conduction. Fig. 14 shows the relation between the (M″) and Log (f) of
Cs/PVA doped 12 ml of AuNPs at 30, 60, 90 and 120 °C. The behaviour of M′ values increases
non-linearly with an increase of frequency, whereas M″ spectra of these films show an electric
modulus relaxation peak. The peak is shifted towards higher frequency with an increase of
temperature. Fig. 15 shows the plot of M' versus M″ for the Cs/PVA-12 ml AuNPs sample at
different temperatures. The presence of the semicircles supports the relaxation processes are non-
Debye behaviour because of the occurrence of different polarization techniques due to the
presence of the external electric field. The variation of the radius is increased related to the
increase of ionic mobility after the addition of AuNPs. The radii of semicircle which founded
confirm the relaxation processes is a non-Debye mechanism and the half semicircles are increased
with the increase of temperature.
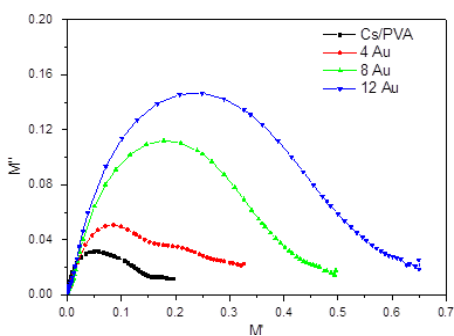
*Fig. 13. The variation of M' with the frequency of the Cs/PVA polymer blend incorporated
by 12 ml gold nanoparticles (AuNPs) at 30, 60, 90 and 120 ℃.*
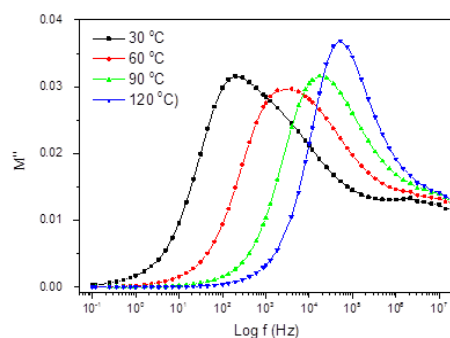
*Fig. 14: The variation of M'' with the frequency of the Cs/PVA polymer blend incorporated
by 12 ml gold nanoparticles (AuNPs) at 30, 60, 90 and 120 ℃.*
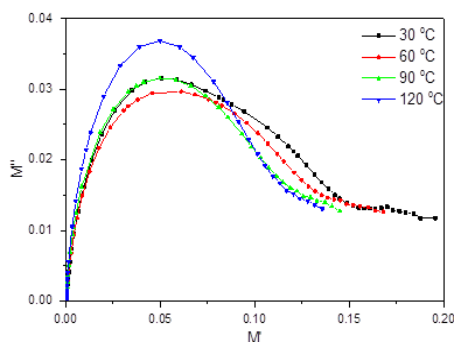
Fig. 15. The variation between M' and M'' of the Cs/PVA polymer blend incorporated by 12 ml gold nanoparticles (AuNPs) at 30, 60, 90 and 120 °C.

4. Conclusion

The detailed of the structural, optical, and dielectric parameters of Cs/PVA–AuNPs nanocomposites were reported. The XRD results confirmed a large reduction in the crystallinity of the nanocomposites after the AuNPs addition and the presence of the main peaks of pure AuNPs with the face centered cubic (FCC) structure. No peaks of AuNPs were observed at low concentrations due to the complete degradation of the AuNPs within the Cs/PVA matrix. The main IR bands of Cs/PVA were recorded. The broad band attributed to the hydrogen bond between OH and NH_2 functional groups was decreased because of the intermolecular interaction between polymer blend and the AuNPs through the formation of coordination interactions with the –OH, C=O group.

The dielectric conductivity, the electrical conductivity and dielectric modulus behaviour were studied by AC impedance method. The values of both ε' and ε'' were decreased as an increase of the frequency and temperature attributed to high contribution of charge accumulation inside the nanocomposites and it was nearly stable at high frequency. The increase in σ_{dc} was discussed according to an increase of the free charge density or of the charge mobility that was a result of Cs/PVA polymer-AuNPs interactions. The radii of the semicircles (Cole-Cole plot) was decreased as the increase of AuNPs indicating to increase of ionic mobility and so the electrical conductivity improvement.

References

[1] P. Sharma, V. Semwal, B. D. Gupta, Photonics Nanostructures - Fundam. Appl. **37**, (2019).
[2] A. A. Menazea, S. A. Abdelbadie, M. K. Ahmed, Appl. Surf. Sci. **508**, (2020).
[3] A. A. Menazea, J. Mater. Res. Technol. **1207**, (2019).
[4] I. S. Elashmawi, N. S. Alatawi, N. H. Elsayed, Results Phys. **7**, 636 (2017).
[5] I. S. Elashmawi, L. H. Gaabour, Results Phys. **5**, 105 (2015).
[6] I. S. Elashmawi, E. M. Abdelrazek, A. M. Hezma, A. Rajeh, Phys. B Condens. Matter. **434**, 57 (2014).
[7] I. S. Elashmawi, N. H. Elsayed, Polym. Bull. **77**, 949 (2020).
[8] M. Dawy, H. M. Rifaat, A. A. Menazea, Chitosan Experimental, 621 (2015).
[9] J. Wang, J. Liang, L. Sun, S. Gao, Chemosphere **219**, 130 (2019).
[10] G. Yuvaraja, J. L. Pathak, Z. Weijiang, Z. Yaping, X. Jiao, Int. J. Biol. Macromol. **103**, 234 (2017).
[11] I. S. Elashmawi, A. A. Menazea, J. Mater. Res. Technol. **8**, 1944 (2019).
[12] R. J. Fong, A. Robertson, P. E. Mallon, R. L. Thompson, The impact of plasticizer and degree of hydrolysis on free volume of poly (vinyl alcohol) films, Polymers (Basel).
[13] T. Siddaiah, P. Ojha, N. O. G. V. R. Kumar, C. Ramu, Mater. Res. **21**, (2018).
[14] Y. X. Zhang, J. Zheng, G. Gao, Y. F. Kong, X. Zhi, K. Wang, X. Q. Zhang, D. X. Cui, Int. J. Nanomedicine **6**, 2899 (2011).

[15] N. Thangamani, N. Bhuvaneshwari, Chem. Phys. Lett. **732**, (2019).

[16] N. Rani, S. Chahal, A. S. Chauhan, P. Kumar, R. Shukla, S. K. Singh, Mater. Today Proc. **12**, 543 (2019).

[17] N. Ahmad, S. Khan, M. M. N. Ansari, R. Bhargava, Mater. Today Proc. **21**, 1735 (2020).

[18] L. H. Gaabour, J. Mater. Res. Technol., 1 (2020).

[19] Y. Yang, R. Xing, S. Liu, Y. Qin, K. Li, H. Yu, P. Li, Carbohydr. Polym. 229, (2020).

[20] Q. Ali, W. Taweepreda, K. Techato, Polym. Test., 82 (2020).

[21] N. M. Deghiedy, S. M. El-Sayed, Opt. Mater. (Amst). 100 (2020).

[22] M. Sabzi, M.J. Afshari, M. Babaahmadi, N. Shafagh, Colloids Surfaces B Biointerfaces, 188 (2020).

[23] L. Das, P. Das, A. Bhowal, C. Bhattachariee, Environ. Technol. Innov., 18 (2020).

[24] S. Choudhary, SnO_2 nanocomposites **5**, 54 (2017).

[25] N. S. Alghunaim, H. M. Alhusaiki-Alghamdi, Phys. B Condens. Matter. **560**, 185 (2019).

[26] S. Lahlali, L. Essaleh, M. Belaqziz, H. Chehouani, A. Alimoussa, K. Djessas, B. Viallet, J. L. Gauffier, S. Cayez, Phys. B Condens. Matter. **526**, 54 (2017).